Supplemental Information for:

Developmental origin dictates interneuron AMPA and NMDA receptor subunit composition and plasticity

Jose A. Matta, Kenneth A. Pelkey, Michael T. Craig, Ramesh Chittajallu, Brian W. Jeffries, and Chris J. McBain

SF1. NMDAR EPSC current-voltage profiles in both neonate and juvenile MGE- and CGE-derived interneurons.

Left, Representative NMDAR-mediated EPSCs were measured 25 ms after the AMPA EPSC peak at –60 mV (red) in 20 mV increments. Middle, the IV plots from NMDA EPSCs shown on left. Right. Averaged IV plots from NMDA EPSCs normalized to the maximum NMDAR EPSC measured at + 40 mV. a. NMDA EPSC from neonatal CGE-derived SC-assc interneuron. b. NMDA EPSC from juvenile CGE-derived SC-assc interneuron. c. NMDAR EPSCs from neonatal MGE-derived basket cell interneuron. d. NMDA EPSC from juvenile MGE-derived basket cell interneuron. N (# cells) = 5, 6, 6, & 7 from 5, 6, 6, &7 slices from 3, 4, 4, 4 animals CGE neonates, CGE juveniles, MGE neonates, & MGE juveniles, respectively.

SF2. sEPSC properties in identified MGE- and CGE-derived interneurons through development.

a. Summary histogram for the sEPSC amplitudes of specified cell type at the neonatal and juvenile stages. b. Histogram of the sEPSC frequencies showing developmental increase in synaptic drive from neonates to juveniles in most cell types examined (MGE-derived basket $p = 0.016$, $dF = 39$, $t = -2.53$; MGE-derived bistratified $p = 0.14$, $dF = 31$, $t = –1.49$; MGE-derived ivy $p = 0.021$, $dF = 16$, $t = –2.6$; CGE-derived basket $p = 0.089$, $dF = 15$, $t = –1.82$; CGE-derived dendrite-target $p = 0.022$, $dF = 25$, $t = –2.44$; CGE-derived SC-assc $p = 0.048$, $dF = 32$, $t = –$

2.03). c. Histogram of the sEPSC rise times. d. Histogram of the sEPSC decay times (fitted with one exponential decay function). MGE Basket neonate: 12 cells from 12 slices from 10 animals; MGE Basket juvenile: 29 cells from 29 slices from 20 animals; MGE Bistratified neonate: 13 cells from 13 slices from 9 animals; MGE Bistratified juvenile: 20 cells from 20 slices from 13 animals; MGE Ivy neonate: 11 cells from 11 slices from 9 animals; MGE Ivy juvenile: 7 cells from 7 slices from 7 animals; CGE Basket neonate: 6 cells from 6 slices from 6 animals; CGE Basket juvenile: 11 cells from 11 slices from 9 animals; CGE Dendrite-targeting neonate: 13 cells from 13 slices from 10 animals; CGE Dendrite-targeting juvenile: 14 cells from 14 slices from 11 animals; SC-associated neonate: 21 cells from 21 slices from 16 animals; SC-associated juvenile: 13 cells from 13 slices from 9 animals. Significant differences in these sEPSC parameters were observed in comparisons between cells grouped by the site of origin. In MGE-derived & CGE-derived cells from neonates the ***sEPSC amplitudes*** were 28.33 ± 1.68 pA (n = 36) and 18.06 ± 1.22 pA (n = 40), respectively ($p = 4.05E^{-06}$). In MGE-derived & CGE-derived cells from neonates the ***sEPSC frequencies*** were 4.28 ± 0.75 Hz (n = 36) and 1.47 ± 0.47 Hz (n = 40), respectively (p = 0.002). In MGE-derived & CGE-derived cells from neonates the ***sEPSC 10-90% rise times*** were 1.08 ± 0.01 ms (n = 36) and 1.37 ± 0.07 ms (n = 40), respectively (p = 0.006). In MGE-derived & CGE-derived cells from neonates the ***sEPSC decay time constants*** were 3.22 ± 0.22 ms (n = 36) and 4.84 ± 0.30 ms (n = 40), respectively ($p = 7.37E^{-05}$). In MGE-derived & CGE-derived cells from juveniles the ***sEPSC amplitudes*** were 24.88 ± 0.15 pA (n = 56) and 16.12 ± 0.83 pA (n = 39), respectively ($p = 7.8E^{-08}$). In MGE-derived & CGE-derived cells from juveniles the ***sEPSC frequencies*** were 9.77 ± 1.04 Hz (n = 56) and 3.16 ± 0.65 Hz (n = 39), respectively ($p = 4.83E^{-06}$). In MGE-derived & CGE-derived cells from juveniles the ***sEPSC 10-90% rise times*** were 1.06 ± 0.04 ms (n = 56) and 1.34 ± 0.07 ms (n = 39), respectively ($p = 2.9E^{-04}$). In MGE-derived & CGE-derived cells from juveniles the ***sEPSC decay time constants*** were 3.27 ± 0.15 ms (n = 56) and 5.22 ± 0.32 ms (n = 39), respectively ($p = 1.2E^{-07}$). *p < 0.05 values from un-paired t-test.

SF3. GluN2 subunit composition in adult CGE-derived interneurons.

a-b. NMDA EPSC in the absence or presence of ifenprodil (ifen; 5μM) from CGE-derived basket cell and CGE-derived SC-assc interneuron, respectively. NMDAR EPSCs in P43 CGE-basket cells continue to possess robust ifenprodil sensitivity and slow kinetics, whereas CGE-derived SC-associated cells show lower ifenprodil sensitivity and more rapid kinetics. c&d. Summary plot for NMDA EPSC decay kinetics ($p = 0.01$, $dF = 11$, $t = 3.1$) and ifenprodil sensitivity ($p = 0.026$, $dF = 11$, $t = –2.55$), respectively. (*$p<0.05$) (data from dendrite targeting cells and CGE-derived basket cells were pooled, 7 cells from 7 slices from 3 animals; and CGE SC-associated, 6 cells from 6 slices from 3 animals).

SF4. Lack of correlation between GluN2 subunit expression and presynaptic transmitter release probability in both MGE- and CGE-derived interneurons.

a&b. Representative traces of pairs of NMDAR EPSCs evoked 75 ms apart in MGE-derived bistratified cells in the absence or presence of ifenprodil (ifen, 5 μM). c. Summary plots of the paired-pulse ratio (PPR, P2/P1) obtained under control or in the presence of ifenprodil for listed cell types (MGE neonate, $p = 0.98$, $dF = 12$, $t = –0.03$, $n = 7$ cells from 3 animals (for control and ifenprodil); MGE juvenile, $p = 0.92$, $dF = 11$, $t = –0.1$, $n = 7$ cells from 7 slices from 3 animals for control and 6 cells from 6 slices from 3 animals for ifenprodil; CGE neonate, $p = 0.89$, $dF = 8$, $t = 0.15$, $n = 5$ cells from 5 slices from 2 animals (for control and ifenprodil); CGE juvenile, $p = 0.99$, $dF = 8$, $t = –0.01$, $n = 5$ cells from 5 slices from 2 animals.

SF5. Synaptic properties of ALV inputs to CGE-derived basket cells remain constant through development.

a&b. Images of representative CGE-derived basket cells recorded in slices from P6 (a) and P18 (b) mice to assay synaptic properties of ALV inputs. During recordings cells were filled with biocytin then fixed and revealed post-hoc by incubating the tissue with Alexa555 conjugated streptavidin. Images are maximum projections of confocal stacks obtained at 20X magnification then converted to grayscale and color inverted. c. Representative traces and summary bar graph illustrating the rectification properties of pharmacologically isolated AMPAR mediated EPSCs evoked by ALV stimulation at holding potentials between –60 to +40 mV (20 mV increments) in P6–P9 and P18–P22 CGE-derived basket cells. d. Representative traces and bar chart summarizing the NMDAR/AMPAR ratios for ALV inputs to CGE-derived basket cells at the developmental periods indicated. e&f. Representative sample NMDAR mediated EPSCS evoked by ALV stimulation in P6 and P18 CGE-derived basket cells before and after ifenprodil treatment. g&h. Bar charts summarizing the decay time constants and ifenprodil sensitivity of ALV evoked NMDAR mediated EPSCs obtained in CGE-derived basket cells at the indicated developmental time points.

SF6. Acute synaptic activity does not drive a GluN2 subunit switch in neonatal CGE-derived interneurons.

a-b. Summary plots of NMDA EPSC decay kinetics (panel a) and ifenprodil sensitivity (panel b) under various conditions: control (panel a: n = 24 cells from 24 slices from 9 animals. Panel b: 13 cells from 13 slices from 9 animals) paired activity = 180 stimulations at 2Hz and holding potential at 0 mV (Panel a: p = 0.88, dF = 29, t = 0.15, n = 7 cells from 7 slices from 3 animals.

Panel b: p = 0.311, dF = 16, t = –1.05, n = 5 cells from 5 animals from 3 animals); unpaired activity (as in figure 4) = 180 stimulations at 2Hz and holding potential at –70 mV (Panel a: p = 0.6, dF = 30, t = –0.53, n = 8 cells from 8 slices from 3 animals. Panel b: p = 0.16, dF = 17, t = 1.46, n = 6 cells from 6 slices from 3 animals); K^+ (as in figure 5) = after enhanced CA3 pyramidal neuron activity with high "K^+" solution (see methods)(Panel a: p = 0.97, dF = 36, t = –0.042, n = 14 cells from 14 slices from 5 animals. Panel b: p = 0.17, dF = 24, t = –1.42, n = 13 cells from 13 slices from 5 animals). Unpaired t-test comparison of various conditions versus control conditions.

SF7. A lack of activity dependent plasticity of NMDARs at alvear inputs onto MGE-derived interneurons.

a-b. Despite the presence of ifenprodil sensitive NR2B containing NMDARs at alvear inputs onto MGE-derived interneurons, neither the synaptic plasticity induction paradigm or exposure to elevated extracellular K (and altered divalents) triggers the change in NMDAR kinetics (panel a; Plasticity: p = 0.87, dF = 10, t = –0.17, n = 6 cells from 6 slices from 3 animals; K^+: p = 0.3, dF = 13, t = 1.07, n = 8 cells from 8 slices from 4 animals) nor a change in ifenprodil sensitivity (panel b; Plasticity: p = 0.87, dF = 10, t = –0.17, n = 6 cells from 6 slices from 3 animals; K^+: p = 0.36, dF = 10, t = –0.95, n = 6 cells from 6 slices from 4 animals) observed at SC inputs onto the same cell population. Unpaired t-test comparison of various conditions versus control conditions (panel a: n = 7 cells from 7 slices from 5 animals. Panel b: 6 cells from 6 slices from 5 animals).

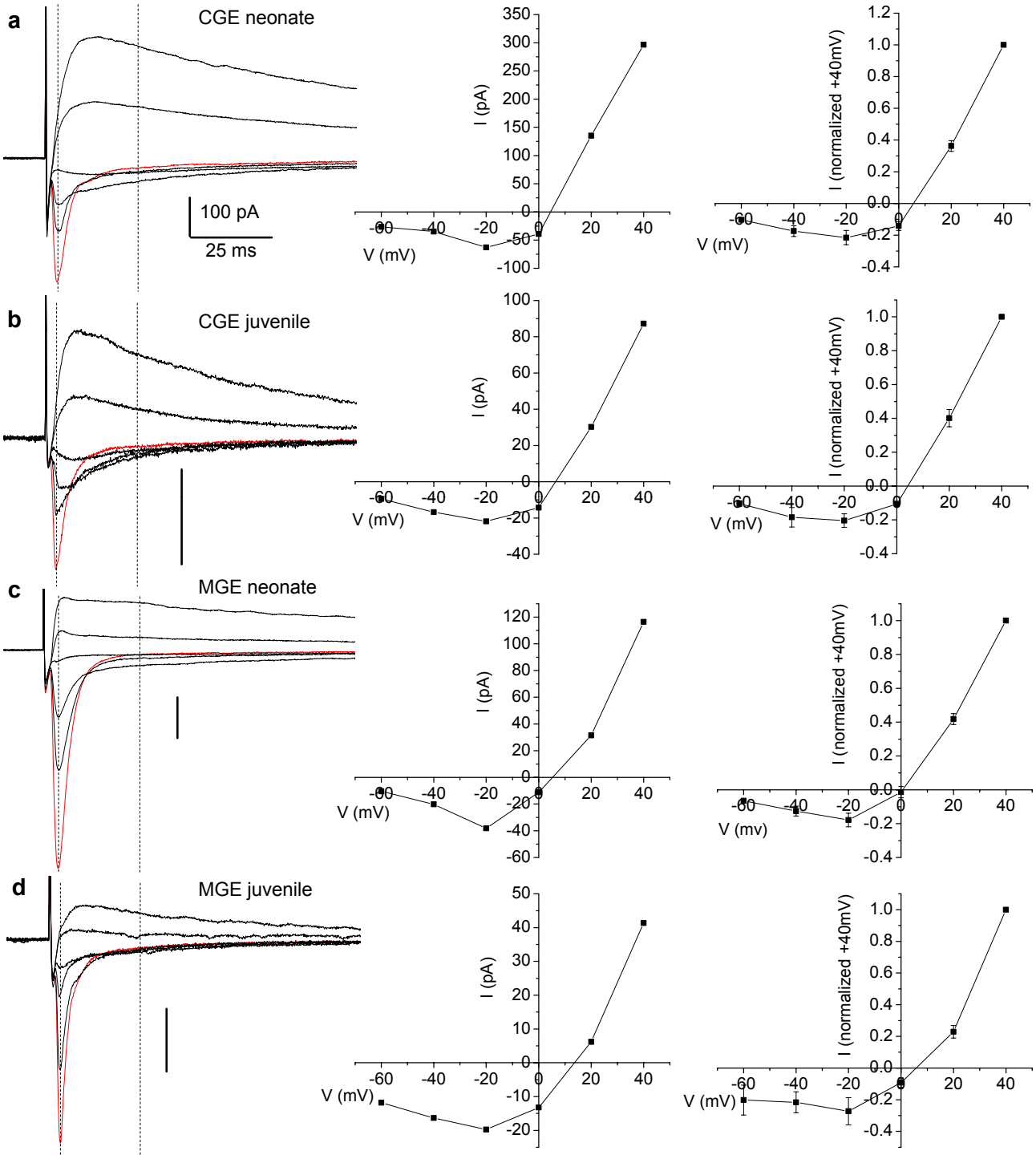

Supplemental figure 1

Nature Neuroscience: doi:10.1038/nn.3459

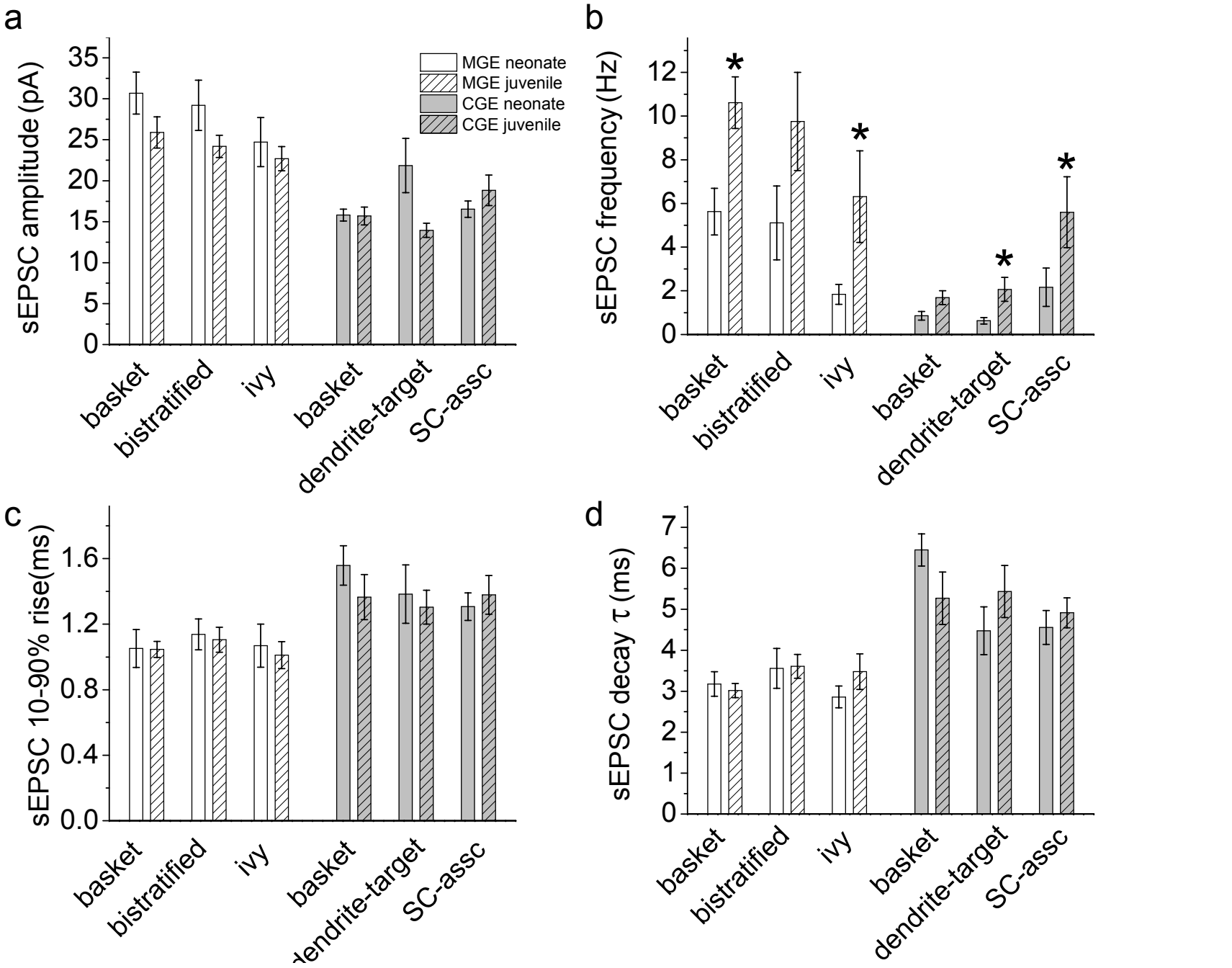

Supplemental figure 2

Nature Neuroscience: doi:10.1038/nn.3459

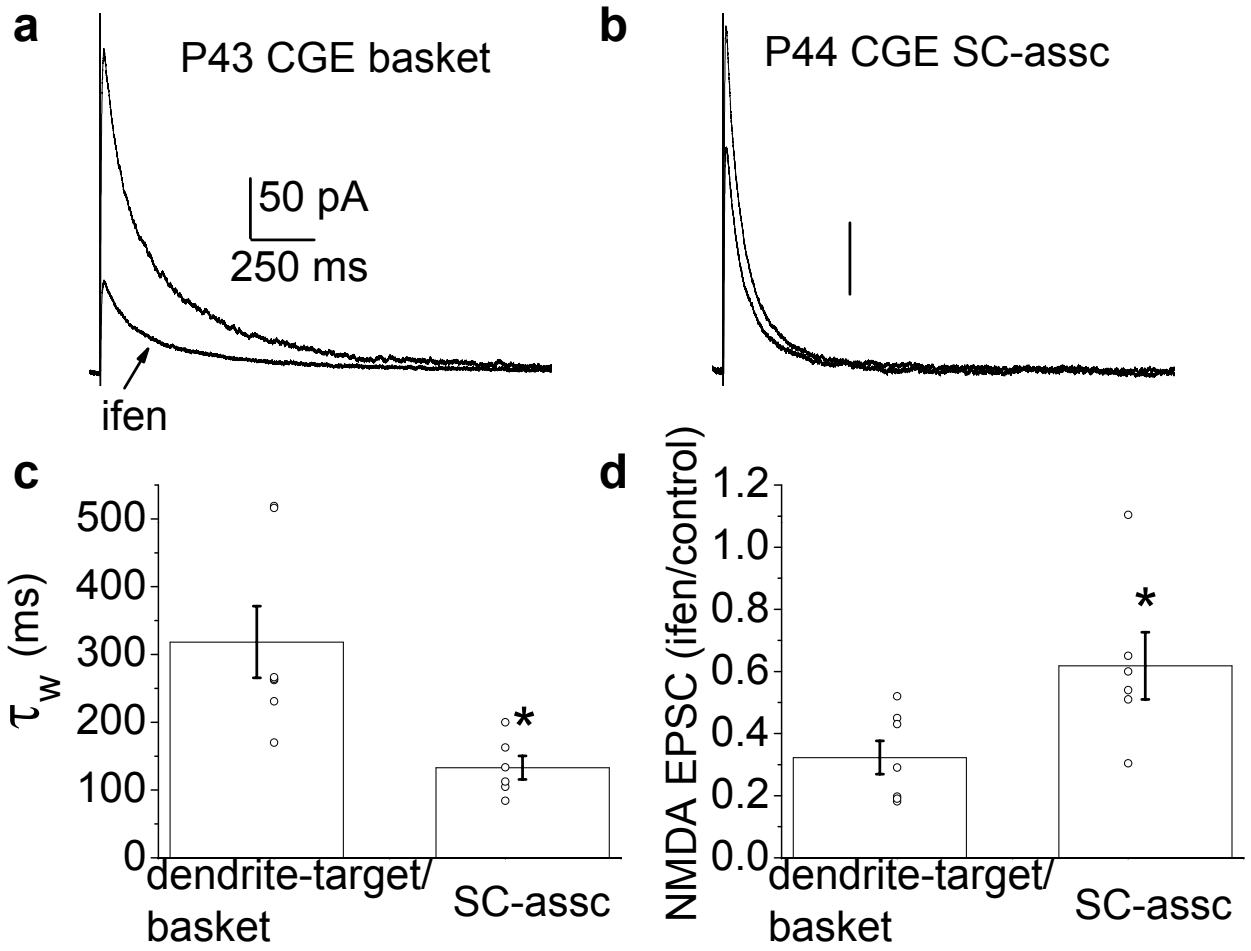

Supplemental figure 3

Nature Neuroscience: doi:10.1038/nn.3459

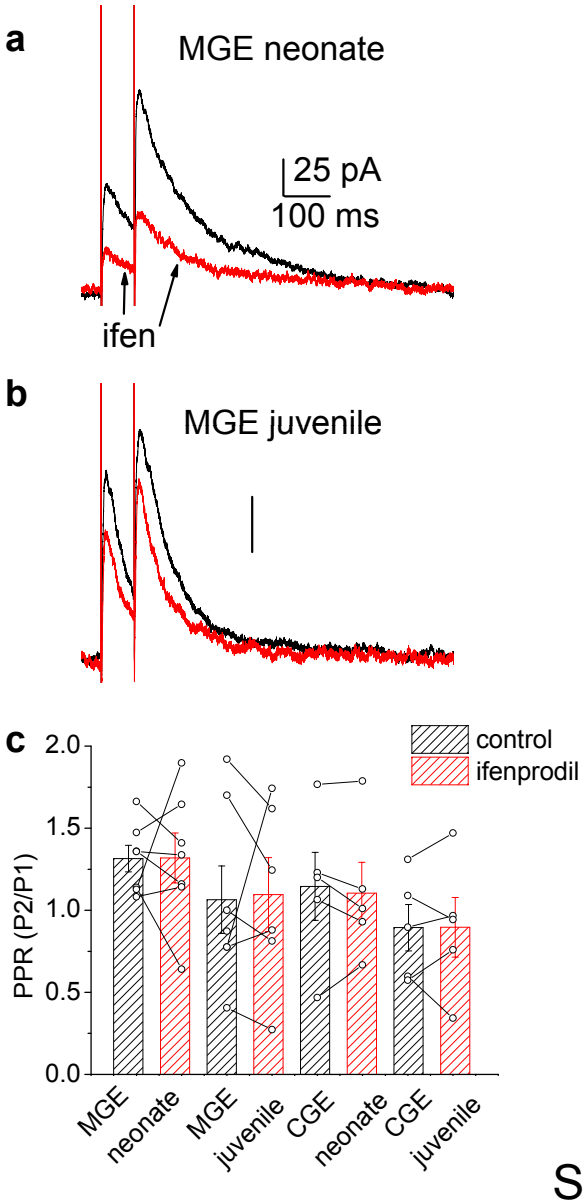

Supplemental figure 4

Nature Neuroscience: doi:10.1038/nn.3459

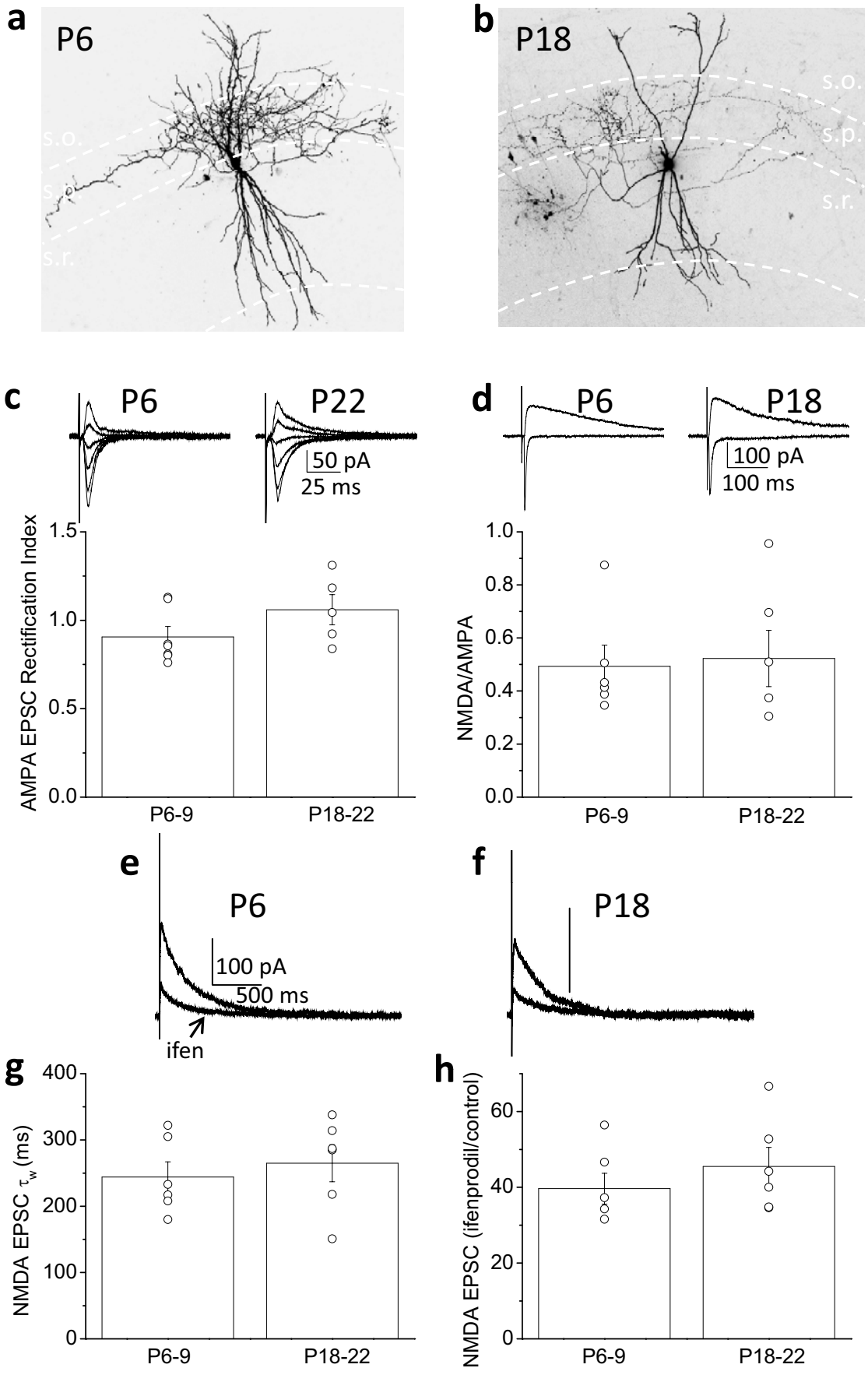

Supplemental figure 5

Nature Neuroscience: doi:10.1038/nn.3459

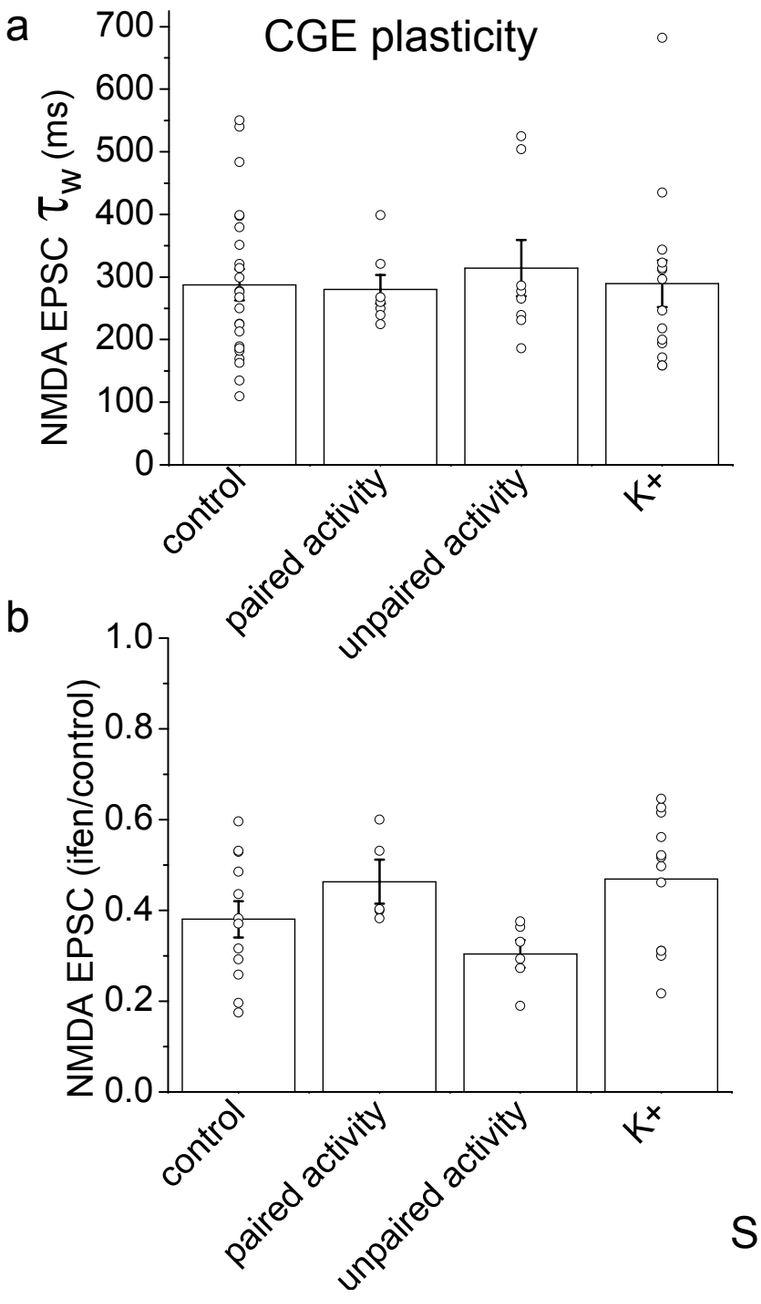

Supplemental figure 6

Nature Neuroscience: doi:10.1038/nn.3459

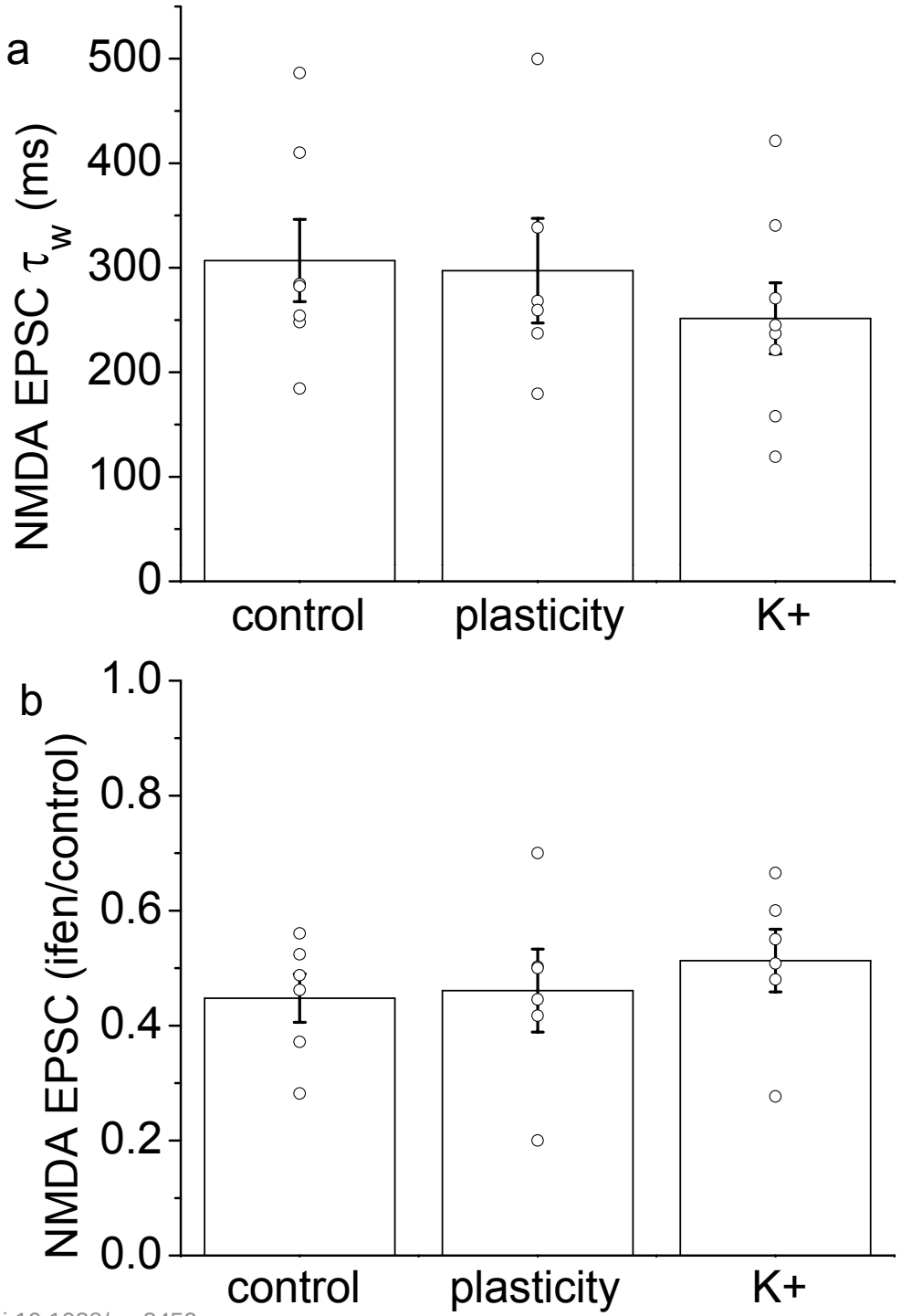

Alveus plasticity

Supplemental figure 7

Nature Neuroscience: doi:10.1038/nn.3459